Alfarama Journal of Basic & Applied Sciences

Faculty of Science Port Said University

https://ajbas.journals.ekb.eg
ajbas@sci.psu.edu.eg
http://sci.psu.edu.eg/en/

ISSN 2682-275X

January 2022 , Volume 3, Issue I DOI: 10.21608/AJBAS.2021.97806.1069

Submitted: 04-10-2021
Accepted: 14-11-2021 Pages: 163-181

Optimization approach for adsorptive removal cationic and anionic dyes using magnetic nanoparticles alginate beads (SP-IONPs-ALG): characterization, isotherm and kinetic modelling

Shymaa M. Shalaby [1,*], Hala Y. EL-Kassas [2]. Adel A. Mohammed [2], Mohamed A. Aly-Eldeen [2], Fedekar F. Madkour[1]

[1] Marine Science Department, Faculty of Science, Port Said University, Egypt

[2] National Institute of Oceanography and Fisheries, Egypt

[*]**Corresponding author**: Shymaashalaby77@yahoo.com

ABSTRACT

Organic dyes are major elements in wastewater effluents, caused serious environmental damage and human health dangers for that we use of factorial design software to evaluate efficiently factors influencing the adsorption capacity of iron oxide nanoparticles alginate beads (SP-IONPs- ALG) to remove crystal violet (CV), methylene blue (MB) and methyl orange (MO) from aqueous solution. The current work included prepared SP-IONPs- ALG by using green synthesized iron oxide nanoparticles (IONPs) using *Spirulina platensis*, then coated by alginate. SP-IONPs- ALG characterized by using EDX and SEM then used it as adsorbent for uptake CV, MB and MO from aqueous solution. A 2^4 (CCD) based on single- factor experiments and a four- variables, pH (x_1), interaction time (x_2), dyes conc. (x_3) and sorbent dosage (x_4) used to evaluate efficiency of SP-IONPs- ALG for adsorption of CV, MB and MO from aqueous solution. The outlined results inferred that pH, contact time and adsorbent dosage had positive effect in dyes remove with high removal percentage for CV, MB and MO (93.46%, 96.47% and 94.4%; respectively). Freundlich model was fitting for description adsorption of CV & MB with maximum adsorption capacity (Q_{max}) 344.82 mg g^{-1}, 416.6 mg g^{-1} respectively but Langmuir isotherm model more fit to describe the experimental data for representing the adsorption process of MO with maximum adsorption capacity 370.3 mg g^{-1}. The kinetic model fitted well with a pseudo second order rate equation. Furthermore, the reusability of SP-IONPs-ALG was successfully achieved by using HCl and NaOH for (CV & MB) and MO, respectively.

Keywords

Iron, nanoparticles, *Spirulina platensis*, *alginate* beads, crystal violet and dyes removal.

1. INTRODUCTION

Recently, dyes manufacturing considers one of the main causes of dangerous environmental defilement that affect aquatic organisms [1]. The dangerous of dyes commonly have complex aromatic molecular structures and have a synthetic origin which give them high stability and hard to biodegradation [2]. The textile industrial discharge treatment has become a huge problem owing to the scarcity of effective device to remove poisonous textile dyes from contaminated wastewater [3]. Huge efforts have been made to improve wastewater treatment with different approaches [4 - 6]. The adsorption systems are presently broadly used to separate pollutants from industrial wastewater due to its numerous advantages as simplicity and high

efficacy [7]. Iron nanomaterials, nowadays have astounding ability for adsorption owing to large surface area, strong magnetic properties and porosity [8]. nanomaterials were synthesised by chemical and physical approaches but many of these methods involve high material, high energy, use of dangerous chemicals and toxic solvents and caused of harmful by-products [9-12]. For that, there is need to improve high-yield, affordable, nontoxic and eco-friendly processes for nanostructures synthesis, so that the biological approaches for synthesis of nanomaterials become vital. Biosynthesis process using microorganisms, algae or plant extracts as alternate operation to synthesis nanomaterials [13].

Naked magnetic nanoparticles have many problems such as the aggregation in water and chemical instability and oxidation. Controversially, it needs huge effort to completely separated from the wastewater through treatment process and recycle in practical applications which have very small particles size. Besides, may be leading to secondary contamination specifically when practical in continual -flow system. To solve these difficulties coating it with a biocompatible shell as alginate [14]. Alginate is a renewable natural polysaccharide containing abundant numerous functional groups such as phenolic and carboxylic for that alginate has been used as green adsorbents to advance their stability & dispersion for green applications [15].

There are in excess of 100,000 kind of dyes that are obtainable, but our existing work concentrated on the crystal violet, methylene blue & methyl orange adsorption onto magnetic nanoparticles alginate bead (SP-IONPs- ALG). Crystal violet, methylene blue and methyl orange used in cosmetic, coloring paper, temporary hair coloring and dying of cotton/wools and commonly found in these effluents. Unfortunately, the uncontrolled utilization of synthetic dyes associated with the broaden industries, has dramatically led to dumping of considerable quantities of dyes laden-wastewater into the aquatic environment [16]. Persistence of these released dyed effluents and/or their decomposition products in the water bodies seriously endanger the health of different living creatures. They deteriorate water quality (specification) by changing chemical propatrties of water, which eventually result in reduce of photosynthesis efficiency due to an increase in the water turbidity associated with reduction of light penetration [17]. These carcinogenic compounds have several health side effects as damages to human eyes, burns, increased sweating and mental disorders [18]. Additionally, it can cause serotonin syndrome, red blood cell breakdown, and allergic reactions [19]. To make sure an effective of sorbent to separate contaminants from wastewater, an optimisation study could be studied [20], the optimisation of the adsorption processes can be achieved by Response Surface Methodology (RSM), which considered as a consolidation statistical with mathematical approach [21]. In actual fact, RSM as an effective method to explain the effectiveness of variables in the defined response along with the relations between all the factors [22]. This method in the optimisation process help to decrease the experiment numeral, process time and cost of adsorption method [23].Thus, the present work has two main objectives: First, develop a biological, cost effective and non-toxic adsorbent magnetic nanoparticles alginate beads (SP-IONPs- ALG) to evaluate the characterization of the (SP-IONPs- ALG) detected by using Energy-Dispersive X-ray (EDX) and Scanning Electron Microscope (SEM). Second, objective is examining the effectiveness of (SP-IONPs- ALG) in adsorption cationic dyes (CV and MB) and cationic dye (MO), tested the variables as experimental time, pH, sorbent dosage and dye concentration by using (RSM). Study the nature of adsorption by EDX and SEM.

1. MATERIALS AND METHODS

2.1. Materials

In the current work was used the green biosynthesized magnetic nanoparticles using *Spirulina platensis* (SP-IONPs) **[24]**. All chemicals were purchased from Merck (Germany). Crystal violet, methylene blue & methyl orange in addition to sodium alginate **(100%)** were obtained from Sigma-Aldrich (Darmstadt, Germany). All solutions were prepared by using deionized water (DW) **(0.05 µS cm^{-1})**.

2.2. preparation of magnetic nanoparticles alginate beads (SP-IONPs- ALG)

In the present study the SP-IONPs- ALG was prepared by encapsulation method for nanoparticles in semipermeable alginate **[25]**, which used to obtain spherical gel beads. SP-IONPs- ALG prepared by desired mass of SP-IONPs in of 4% (w/v) sodium alginate solution. Stirred for 30 min, the solution extruded as small drops into a stirred solution of 3.5 % calcium chloride to obtain a homogeneous mixture, wherever 2.3 mm round shape gel beads were formed. Finally, beads allowable to harden, then washed by DW.

2.3. Physical and morphological characterization of SP-IONPs- ALG

The microanalysis structure of SP-IONPs- ALG was detected by the EDX spectrum using an X-ray micro-analyzer (Module Oxford 6587INCA X-sight) for distinguished the elemental composition. Surface morphology of SP-IONPs- ALG was determined by using Scanning Electron Microscopy (SEM) JEOL (JSM-6510LV). SP-IONPs- ALG zeta potential (pH_{PZC}) was examined by plotting a graph of ΔpH ($pH_{eq} - pH_0$). (0.05 g) of SP-IONPs- ALG adsorbent was added to 10 mL of 0.1 M NaCl for 24 hours with varying the (pH_0) between 1 to 12. The ending pH (pH_f) was noted and the pH PZC coincide to $pH_0 = pH_f$.

2.4. Dyes solutions preparation

CV, MB & MO dyes stock solutions were prepared by dissolving suitable quantities of dyes in DW to final concentrations (C_0; 1000 mg L^{-1}), then dilute by DW to preparing the experimental solutions. HCl and NaOH were used for pH amendment.

2.5. Batch experimental studies

A batch equilibrium method was performed at different adsorption conditions. The physicochemical variables: pH (2 - 10), initial dye concentration (10 - 1000 mgL^{-1}), adsorbent dose (0.02 - 0.1 g), contact time (3 - 180 min.). The effectiveness of sorbent dose on dyes removal was examined by varying the adsorbent dose from 0.02 to 0.1 g were added separately to each CV, MB and MO experimental solutions at room temperature (℃; 25 ± 1) for 90 min. Designed for adsorption isotherms, SP-IONPs- ALG (0.05 g) was added to 20 mL of various dyes concentration ranging between (C_0; 10 - 1000 mgL^{-1}) at 120 rpm for 90 min in rotary shaker (VELP SCENTIFICA). Dyes concentrations were determined by double-beam spectrophotometer (JENWAY 6800 UV/VIS). Crystal violet was measured at wavelength 590 nm [26], methylene blue at 664 nm [27] and methyl orange at 463 nm [28]. The adsorbed quantity of dyes expressed as (q_{eq}) and the removal percent detected on the word of the following (Eq.1&2) respectively:

$$q_{eq} = \frac{(C0 - Ce)V}{m} \quad \textbf{(1)}$$

$$R \quad (\%) \quad = \frac{Co - Ce}{Co} \times 100 \quad \textbf{(2)}$$

Wherever; C_0 (mg L^{-1}) is initial dyes samples absorbance at equilibrium and C_e (mg/ L) is measured dyes samples absorbance at equilibrium. V is the solution volume (L), and *m* is the sorbent dose (g).

2.6. Factorial Experimental Design

In the present study, (CCD) with single-factor experiments and a four-variables, pH (x_1) 2 - 10, contact time (x_2) 5- 65 minutes, the initial dyes concentration (x_3) 5 – 105 mg L^{-1} and sorbent dose (x_4) 0.02 – 0.1 g, which considered as the independent variable used to evaluate the efficiency of SP-IONPs- ALG for removal of CV, MB & MO dyes from aqueous solution. The adsorption experiments were showed randomly at various levels of independent variables coded as $+\alpha$, +1 and –1, $-\alpha$ for higher and lower values with six central points to give 30 experimental runs can be achieved at the similar time. The lower and higher levels for the factors were designated along with previous experiments. The ranges and levels of these independent variables investigated are presented in Table (1). All probable amalgamations of these variables were used, and a matrix was recognised consistent with their higher and lower levels as defined in Response Surface

Table 1. CCD matrix of four independent variables affecting CV, MB and MO removal efficiency by SP-IONPs-ALG and their observed response.

Independent variables			Ranges and coded				
Factors	coded	Unites	-α (-2.0)	Low (-1)	middle (0)	High (1)	+α (+2.0)
pH	*X1*	-	2	4	6	8	10
Contact time	*X2*	min	5	20	35	50	65
Initial concentration	*X3*	g	5	30	55	80	105
Adsorbent dosage	*X4*	mg L^{-1}	0.02	.04	0.06	0.08	0.1
Run order	Adsorption variables				Response		
	X1	*X2*	*X3*	*X4*	R% CV	R% MB	R%MO
1	0	0	0	0	56.50	74.65	61.64
2	0	0	+α	0	68.59	50.74	59.73
3	+1	+1	+1	+1	61.28	84.42	45.12
4	-α	0	0	0	30.38	23.82	91.60
5	+1	-1	-1	-1	66.11	81.61	31.93
6	0	0	0	+α	80.61	75.42	74.17
7	-1	+1	+1	+1	56.99	30.44	81.88
8	0	0	0	0	61.59	74.12	57.19
9	+1	+1	-1	-1	55.97	83.32	46.62
10	+α	0	0	0	50.58	92.21	31.84
11	0	0	0	0	59.77	77.17	59.24
12	0	0	0	0	60.68	76.26	57.87
13	+1	-1	-1	+1	84.48	86.66	38.82
14	+1	+1	-1	+1	80.99	89.81	54.13
15	0	0	0	0	60.68	73.66	58.21
16	+1	-1	+1	+1	67.21	92.96	59.25
17	0	0	0	0	60.41	74.58	60.61
18	0	0	-α	0	93.46	96.47	94.4
19	-1	-1	-1	-1	52.81	58.53	69.31
20	0	+α	0	0	79.88	83.13	65.82
21	0	-α	0	0	49.58	57.78	54.79
22	-1	+1	-1	-1	47.90	60.41	76.96
23	+1	+1	+1	-1	53.64	68.63	42.92
24	0	0	0	-α	44.67	66.18	54.45
25	-1	-1	+1	+1	55.81	53.13	79.62
26	-1	-1	+1	-1	47.64	49.89	61.09
27	-1	+1	+1	-1	60.71	52.85	79.99
28	+1	-1	+1	-1	73.85	60.95	63.47
29	-1	-1	-1	+1	47.58	58.53	77.72
30	-1	+1	-1	+1	66.58	60.41	84.75

Methodology (RSM) (Table 1). The responses of variables were calculated by the following equation [29].

$$Y = \beta 0 + \sum_{i=1}^{k} \beta i X i + \sum_{i=1}^{k} \beta i i X_i^2 + \sum_{i=1}^{k-1} * \sum_{i=1+1}^{k} \beta i j X i \, X j \quad (3)$$

Wherever; Y shows the response of variable (CV, MB & MO adsorption), X_i and X_j are independent coded variables and β_0, β_i, β_{ii}, β_{ij} are the intercept term linear, quadratic and interaction effects, respectively [30].

2.7. Adsorption isotherm modelling

The Adsorption isotherms of CV, MB and MO onto SP-IONPs- ALG was analysed using various isotherm models; Langmuir and Freundlich isotherms [31,32] which used for fit CV, MB & MO dyes removal data. The Langmuir isotherm expressed by (Eq.4).

$$\frac{Ce}{Qe} = \frac{1}{qm\,KL} + \frac{C}{qm} \quad (4)$$

Wherever; Q_e, adsorption capacity at the equilibrium; q_m & K_L Langmuir constants, C_e is the adsorbate concentration (mg L^{-1}). The Langmuir constants q_m & K_L were evaluated from the slope and intercept of the linear equation.

The Freundlich isotherm expressed by Equation (5):

$$logQe = \frac{1}{n} logCe + logKf \quad (5)$$

Wherever; Q_e is the SP-IONPs- ALG adsorption capacity (mg g^{-1}); C_e is the adsorbate concentration of; K_f & n is the Freundlich constant.

2.8. Adsorption kinetics modelling

Pseudo-first-order (PFORE) and pseudo-second-order (PSORE), used for explain dyes adsorption kinetics [33- 34]. For adsorption kinetics experiments, SP-IONPs- ALG (0.1 g) was added to 200 mL of mentioned dyes solutions for 90 minutes (C_0; 100 mg L^{-1}) at 120 rpm. Different samples (5mL) were collected at various contact times, then dyes concentrations were determined. The SP-IONPs- ALG quantity of CV, MB & MO per weight unit of adsorbent at experimental time t($q_{(t)}$) was detected by (Eq.6).

$$q(t) = \sum_{i=1}^{n} \frac{(C(t)i-1 - C(t)i) x V(t)(i-1)}{m} \quad (6)$$

where $C(t)_{(i)}$ is the concentrations of CV, MB and MO (M) at time *t*, $C(t)_{(0)} = C_0$, $V(t)_{(i)}$ (mL) is the volume of the solution in the flask at sample number *i*, time *t* and *m* is the mass of the adsorbent in the flask. The sample volume $V(t)_{(i)} - V(t)_{(i-1)}$ equals 5mL.

t

2.9. Regeneration and reusability studies

Desorption study was used to estimate the economic issue of the used adsorbent in the adsorption processes. In this work, reusability study is done by adding sorbent amount (0.1 g) to 20 mL of dyes solutions (C_0; 100 mg L^{-1}) at room temperature (℃ 25 ± 1) for 90 min, then separate the loaded adsorbent from solution by magnetic attraction, the loaded particles were dried at 60 ℃ for 1 hr. Dry SP-IONPs- ALG immersing in 0.1M NaOH and 0.1M HCl concentration for (CV & MB) and MO, respectively at room temperature (℃ 25 ± 1) for 60 minutes. The regenerated adsorbent was washed by deionized water then complete drying at 100 °C (2 hr) for the following run [35]. The process was recurrent for four cycles, then removal efficacy was measured by Eq.7.

$$\text{Regeneration efficiency (\%)} = \frac{\textbf{Amount of desorbed}}{\textbf{Amount of adsorbed}} \times 100 \quad (7)$$

3. Results and Discussion

3.1. Characterization of SP-IONPs- ALG

Formed SP-IONPs- ALG beads have round shape and brown colour due to the iron oxide nanoparticles existence. By comparison between wet and dried beads particle size, the SP-IONPs- ALG adsorbents displayed significant shrinkage after drying as appearance in Figure (1). The diameters of wet and dry SP-IONPs- ALG beads is 3.5 mm and 2.3 mm, respectively [36], The SEM images for the SP-IONPs- ALG beads are revealed in Fig. 2 a, as shown, a porous structure was clearly observed for all the beads. The composition of the magnetic alginate beads was also detected by the Energy-dispersive X-ray spectrum (EDS) (Fig. 2 b), where the iron (Fe), oxygen (O), carbon (C), sodium (Na), sulphur (S) were detected. Presence of iron (63.12 %) and Oxygen (18.03) is related to the present of iron oxide nanoparticles. Also, Sodium (0.72 %) is originated from sodium alginate precursors used in the formation protocol [37].

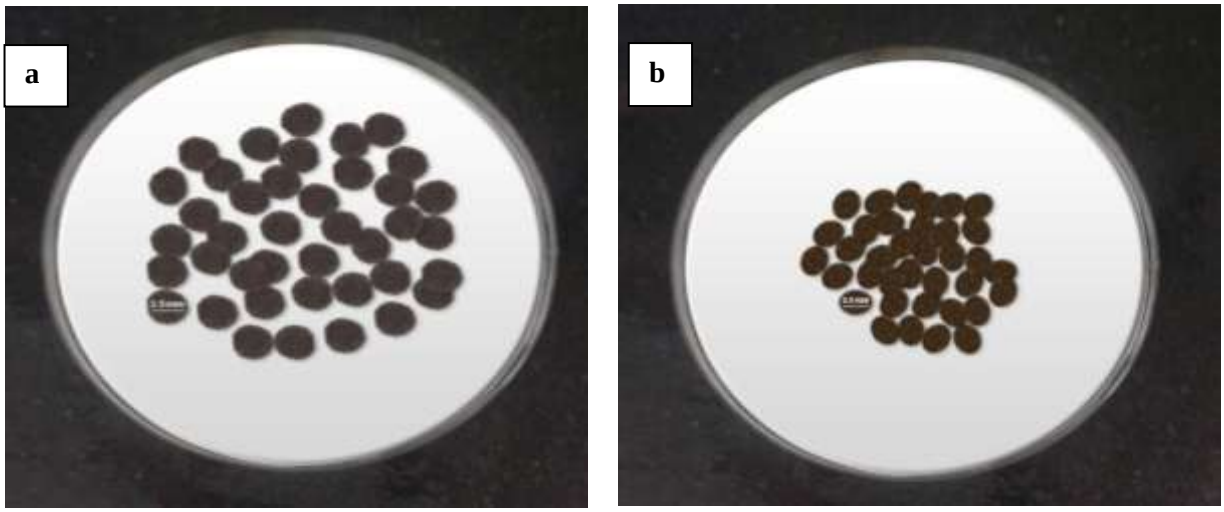

Figure 1. photographic of SP-IONPs- ALG beads (a) Wet beads (b) Dry beads

EDX and SEM analyses were also carried out after loading of CV, MB and MO onto SP-IONPs- ALG. The structural features of adsorbent after adsorption were different, CV, MB and MO were appeared as aggregates on the surface of it (Fig 2 b, c and d). EDX measurements were also slightly affected, indicating the adsorption of dyes molecules onto adsorbent. The structure of SP-IONPs- ALG after loading the three dyes were characterized by EDX as shown in Figures (2 b, c and d). The detection of N with an increase in C and Cl for CV and finding of O, Fe, C, Cl, Na for MB and N, Na and S for MO dyes, all that related with the chemical structures of the mentioned dyes. Additionally, the weight of Fe was decreased for all dyes due to the trapped dyes molecules which contains aromatic rings. These results indicate the strong interaction between dyes and nanoparticles [38].

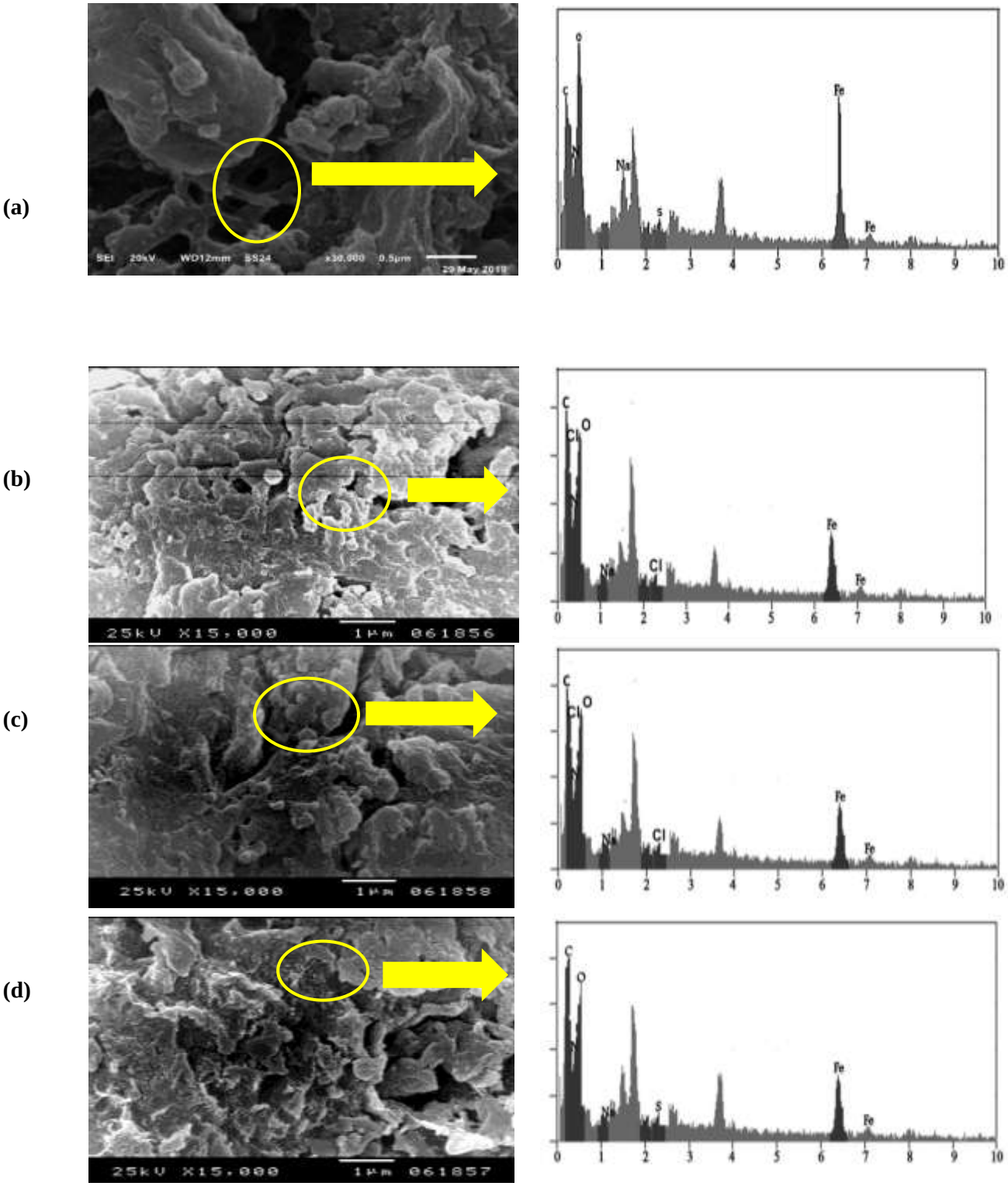

Figure 2. Scanning Electron Microscope (SEM) and Energy Dispersive X-ray spectroscopy (EDX) **(a)** SP-IONPs- ALG, **(b)** after loading CV **(c)** after loading MB **(d)** after loading MO**.**

3.2. Effect of various experimental factors

The pH of solution is significant parameter in the adsorption process which mainly accompanying with the charge on the sorbent surface [39]. Influence of pH values on the CV, MB & MO dyes adsorption

onto SP-IONPs- ALG adsorbent was obtainable in Fig 3a. The adsorption of the cationic dyes, it was slowly increased at pH_0 = 2 - 10, giving the low adsorption capacity 31.5 and 23.19 mg g^{-1} (R% =78.9-57.9 %) for CV & MB, respectively in acidic medium pH 2. The adsorption capacity slight increase to 38.8 – 35.6 mg g^{-1} (R = 97.08 – 89.06 %) at pH 10. This behaviour is due to that the increase pH (i.e., at basic solutions), Strong electrostatic connections happened between the negative charged of SP-IONPs- ALG at pH < 7.1 and positive charged groups of CV & MB that led to adsorption capacity improvement [40]. Instead, the adsorption capacity of MO higher in the acidic medium, which recorded 39.5 mg g^{-1} (R% = 98.8%) at pH 2, the electrostatic interaction between positive charge of sorbent and dye anions increased at acidic solution, leading to the increase of adsorption capacities [41].

The pH effect on the dye removal may be because of pH_{PZC} of adsorbent. Surface charge of adsorbents is neutral, negative and positive according to pH_{PZC} value [42]. The point of zero charge (pH_{PZC}) of the SP-IONPs- ALG beads performed in distilled water was found to be 7.1 illustrated in Fig 3b. These results explained high adsorption capacity of adsorbent with cationic dyes (CV and MB) in alkaline medium and high adsorption capacity of it with anionic dye (MO) in acidic medium [43].

Figure (4 a) illuminated the adsorption capacity of SP-IONPs- ALG, pH equal 10 and 2 for remove (CV & MB) and MO respectively from aqueous solution by varying the sorbent dose (0.01 - 0.1 g). The adsorption capacity of CV, MB and MO increased from 31.2, 30.9 mg g^{-1} and 35.4 to 39.8, 38.1 and 38.9 mg g^{-1} respectively along with increasing sorbent dosage. Higher adsorption capacity which based on the more available surface sites and free sites seemed with increase the sorbent dose [44]. As illustrated in Figure (4,c) it was observed that the adsorption capacity of CV, MB and MO onto SP-IONPs- ALG adsorbent dramatically escalated with an increasing of dyes concentration. At lower dyes concentration, the adsorption sites of adsorbent's surface weren't fully interacted with CV, MB and MO dyes molecules, while they gradually saturated with an increase in the concentration of CV, MB and MO up to the saturation point [45].

(a)

(b)

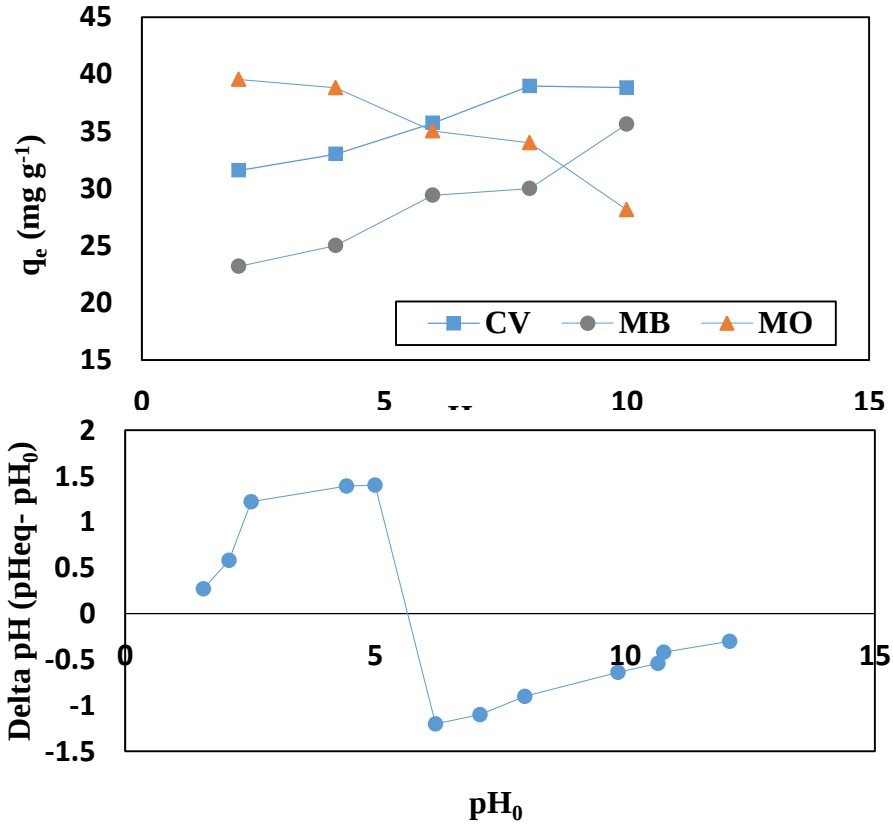

Figure 3. (a) The effect of pH on the adsorption of crystal violet (CV), methylene blue (MB) and methyl orange (MO) onto SP-IONPs-ALG and **(b)** Representation of ΔpH (pH_{eq}–pH_0) versus initial pH (pH_0) for SP-IONPs- ALG adsorbent (C_0: 20 mg L^{-1}; T: 25 ± 1 °C; t: 90 min; m: 0.05 g L−1 ; V: 10 mL).

3.3. Adsorption kinetics

adsorption kinetics is importance for defining the numerical adsorption appearances as adsorption rate and rate-controlling step. Examining the effect of operational time on the CV, MB and MO adsorption process by using SP-IONPs- ALG adsorbent is useful for understand the nature of adsorption process. Adsorption kinetics was achieved to describes the reaction paths and recognise the adsorption process then expecting the adsorption rate with the equilibrium time. chemical kinetics clarified adsorption mechanism with explain the effects of chemical and physical properties of adsorbent and adsorbate on it [46].

In order, the adsorption process was practiced at several concentrations (10 to 1000 mg L^{-1})with adsorbents dose 0.05 g at °C; 25±1 and pH 10 with different contact time 3 - 180 minutes. Apparently, the relative rapid adsorption rate (~ 97% at first 15 min) could be elucidated by the excessive availability of the unoccupied adsorptive sites [47]. Particularly, with going on with the operational time, the sorption rates became slower until the equilibrium was attained for CV, MB and MO after 30 minutes, then a steady trend seems in the adsorption curve as shown in Figure (4b).

(a)

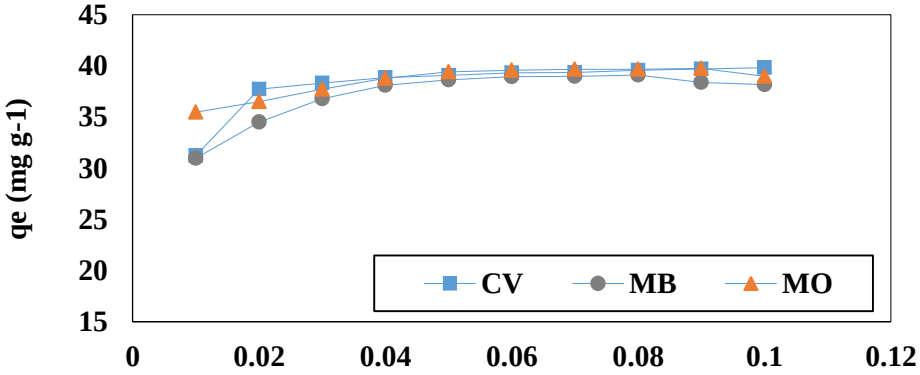

(b)

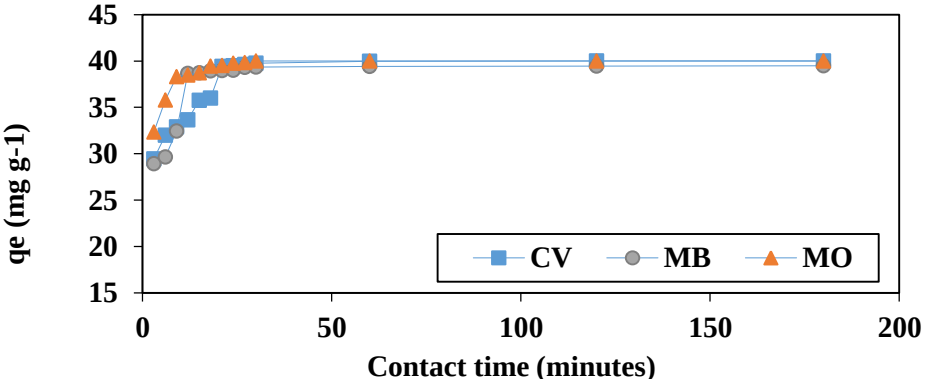

(c)

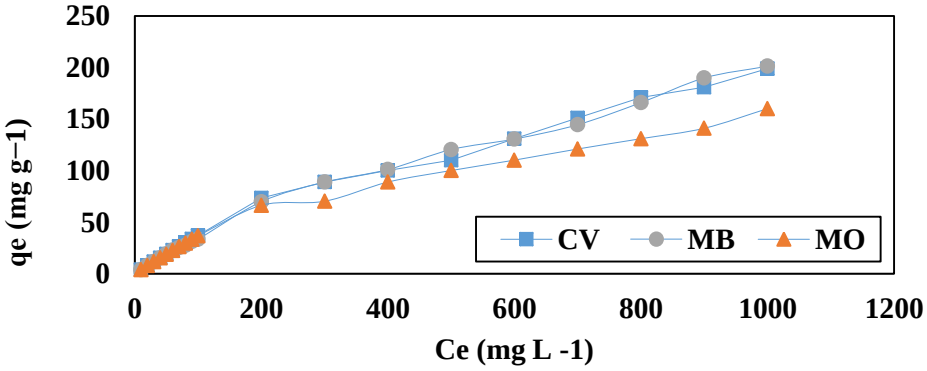

Figure 4. (a) Effect the adsorbent dose of SP-IONPs- ALG on the crystal violet, methylene blue and methyl orange adsorption ($C_{0;}$ 100 mg L^{-1}; T 27 ± 1 °C; volume; 20 mL; pH; 10) and **(b)** Effect of contact time on

the crystal violet, methylene blue and methyl orange adsorption onto SP-IONPs- ALG (C_0; 100 mg L^{-1}; pH; 10; volume; 20 mL; adsorbent mass; 0.05 g).**(c)** Effect of initial concentration on the crystal violet, methylene blue and methyl orange adsorption onto SP-IONPs- ALG (pH; 10; volume; 20 mL; adsorbent mass; 0.05 g).

Experimental data was fitted into pseudo first order rate equation (PFORE) and pseudo second order rate equation (PSORE) were the most commonly applied models to investigate the rate of constant and order of adsorption [48]. The (PFORE) and (PSORE) were also used to fit the experimental data obtained from the batch experiments. Figure 5 a and b was shown the kinetic constants obtained by linear regression of the two models. The Experimental data demonstrated good agreement of experimental values of q_e (39.99, 39.42 and 39.99 mg g^{-1}) nearly close to calculated ones (22.8, 29.58 and 31.84) with high R^2 value (0.942, 0.946 and 0.966 mg g^{-1}) for CV, MB and MO, respectively with pseudo - second - order providing evidence that the adsorption of CV, MB and MO on adsorbents followed pseudo-second order kinetic model. .

(a)

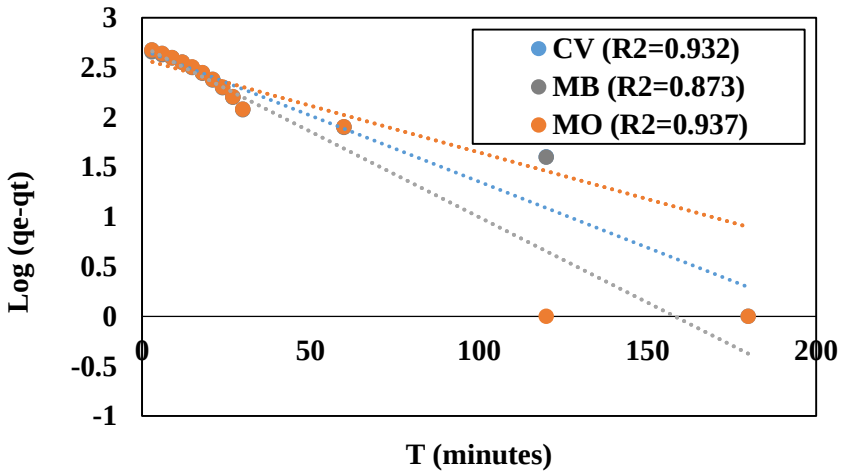

(b)

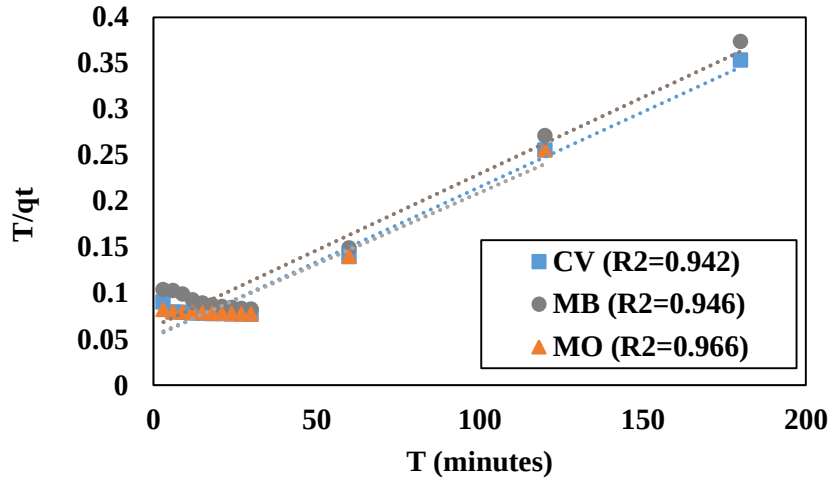

Figure 5. (a) The Pseudo-First-order kinetics of adsorption CV, MB and MO onto SP-IONPs- ALG and **(b)** the Pseudo-Second-order kinetics of adsorption CV, MB and MO onto SP-IONPs- ALG **(**C0: 100 mg L^{-1} ; T: 25 ± 1 ^{o}C; t = 90 min; V: 200 mL; m: 0.1 g).

3.4. adsorption isotherm

In actual, the isothermal analysis is essential to deliver significant information characterized to adsorbent surface properties; it's affinity to provide useful information about the interactive behaviour

between the adsorbent and adsorbate for expecting adsorbent adsorption capacity and understand adsorption mechanism. therefore, could showed the distribution of adsorbate molecules between the liquid and solid phase [49]. adsorption isotherm were studies with various initial concentrations of dyes (C_0, 10- 1000 mg L^{-1}) at room temperature (℃; 25±1). Langmuir and Freundlich isotherm models applied to described experimental data, as shown in Figure (6 a & b). Through comparing the correlation coefficient (R^2) recorded from the mentioned models (Table 2), the high R^2 value 0.988 and 0.974 for CV and MB, respectively. Freundlich model was more fit to the description adsorption of CV and MB onto the SP-IONPs- ALG. Maximum adsorption capacities of SP-IONPs- ALG were reported to be (Q_{max}) 344.82 mg g^{-1}, 416.6 mg g^{-1} for CV and MB respectively. Its results similar to pervious study described by Nadia et al. [50]. Based on the obtained coefficient of determination (R^2) 0.966, SP-IONPs- ALG obeys Langmuir isotherm more fit to experimental data for representing the adsorption process of MO. Maximum adsorption capacity of adsorbent was reported to be 370.3 mg g^{-1}. . It can be summarized that as prepared adsorbent definitely exhibited superior CV, MB and MO dyes separation efficiencies over the previously reported adsorbents [24, 51].

(a)

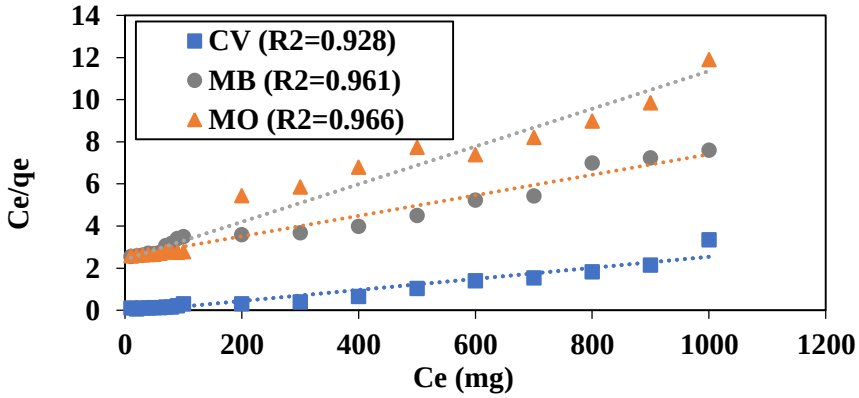

(b)

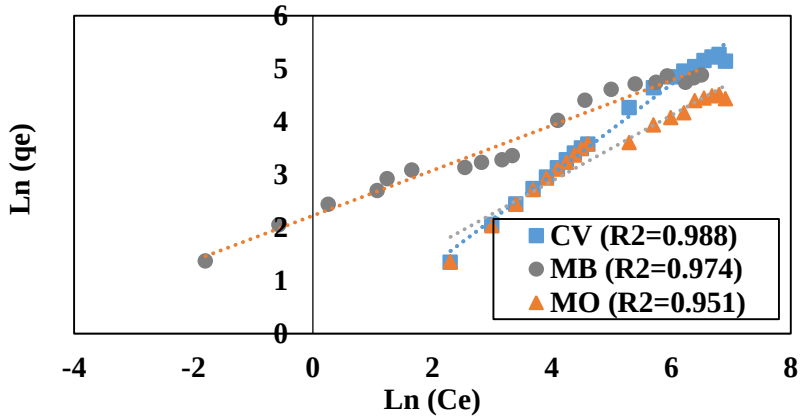

Figure 6. Adsorption isotherm of CV, MB and MO onto SP-IONPs- ALG **(a)** Langmuir isotherm **(b)** Freundlich isotherm(T: 25 ± 1 ^oC; t = 90 min; V: 20 mL; m: 0.05 g).

Table 2. Isothermal parameters for the sorption of CV, MB and MO dyes onto SP-IONPs- ALG adsorbent

Isothermal model	CV	MB	MO
Langmuir)			
K_L (L mg^{-1})	0.0029	0.0027	0.0027
R^2	0.928	0.961	0.966
Freundlich			
N	1.097	1.192	1.82
R^2	0.988	0.974	0.951

3.5. Optimization of CV, MB and MO uptake conditions by applying Response Surface Methodology (RSM)

RSM is showed in Table 1, four independent variables (pH, experimental time, concentration and sorbent dose). These experimental runs were used to evaluate the efficiency of SP-IONPs- ALG for removal CV & MB as cationic dyes and MO as anionic dye and the percentage removal (response) for each combination of the process variable, was involved in the RSM approach to recognize the interaction of each variable on the response. Amongst the 30 experiments, 6 experiments were repetition of the central point (run Nos. 1, 8, 11, 12, 15 and 17). The nearness of 6 experiments responses can be confirmed the accuracy of the experiment process [52]. The experimental results for CV removal were fitted in Quadratic model which R^2 equal 0.928 and adjusted R^2 equal 0.860 but MB and MO were fitted in Linear model which R^2 equal (0.7556 - 0.7110) and adjusted R^2 (0.7165 - 0.6647) respectively. ANOVA for statistical analyses values of CV, MB and MO less than 0.0001, these results indicate these models' terms are significant, these results illustrated in Tables 3, 4 and 5.

In the current work, the highest percentages CV, MB & MO removal by the CCD method were obtained in run No. 18, which the percentages equal 93.46%, 96.47% and 94.4%; respectively but the lower removal percentage of them obtained in run 4 for CV and MB 30.38% and 23.82% respectively and run 5 for MO which percentage was 31.9%, these results were shown in Table 1. In the run No.18 pH equal 6, contact time (t; 35 minutes), initial concentration (C_0; 5 mg L^{-1}) and sorbent dose (0.06 g), the higher dyes removal percentage in this run could be owing to the lower dyes concertation, the similar results described by Priya et al. [53].

Table 3. ANOVA for Quadratic model of crystal violet removal by SP-IONPs-ALG

	Sum of Squares	df	Mean Square	F-value	p-value	
Model	4068.65	14	290.62	13.80	< 0.0001	Significant
A-pH	98.27	1	98.27	4.67	0.0473	
B-Time	0.0962	1	0.0962	0.0046	0.9470	
C-Conc.	1196.13	1	1196.13	56.81	< 0.0001	
D-Dose	1154.00	1	1154.00	54.81	< 0.0001	
AB	420.85	1	420.85	19.99	0.0004	
AC	37.28	1	37.28	1.77	0.2032	
AD	2.59	1	2.59	0.1229	0.7308	
BC	14.72	1	14.72	0.6992	0.4162	
BD	3.03	1	3.03	0.1437	0.7099	
CD	322.69	1	322.69	15.33	0.0014	
A^2	172.81	1	172.81	8.21	0.0118	
B^2	259.85	1	259.85	12.34	0.0031	
C^2	305.28	1	305.28	14.50	0.0017	
D^2	32.40	1	32.40	1.54	0.2338	
Fit Statistics						
Source	Std. Dev.	R^2	Adjusted R^2	Predicted R^2	PRESS	
Linear	8.80	0.5584	0.4878	0.3297	2938.99	
2FI	7.73	0.7412	0.6049	0.4594	2370.15	
Quadratic	4.59	0.9280	0.8607	0.6629	1478.01	Suggested
Cubic	3.39	0.9817	0.9241	0.9272	319.01	Aliased

Table 4. ANOVA for Linear model of methylene blue removal by SP-IONPs- ALG.

Source	Sum of Squares	df	Mean Square	F-value	p-value	
Model	6504.72	4	1626.18	19.32	< 0.0001	Significant
A-pH	4942.21	1	4942.21	58.73	< 0.0001	
B-Time	118.08	1	118.08	1.40	0.2473	
C-Conc.	1285.95	1	1285.95	15.28	0.0006	
D-Dose	158.48	1	158.48	1.88	0.1822	
Fit Statistics						
Source	Std. Dev.	R^2	Adjusted R^2	Predicted R^2	PRESS	
Linear	9.17	0.7556	0.7165	0.6271	3210.41	Suggested
2FI	9.07	0.8186	0.7231	0.4678	4581.35	
Quadratic	9.16	0.8537	0.7171	0.2160	6748.76	
Cubic	5.98	0.9710	0.8797	-1.2426	19304.96	Aliased

Table 5. ANOVA for Linear model of methyl orange removal by SP-IONPs- ALG.

Source	Sum of Squares	df	Mean Square	F-value	p-value	
Model	372.85	4	93.21	15.37	< 0.0001	Significant
A-pH	298.25	1	298.25	49.19	< 0.0001	
B-Time	5.64	1	5.64	0.9298	0.3441	
C-Conc.	61.40	1	61.40	10.13	0.0039	
D-Dose	7.57	1	7.57	1.25	0.2746	
Fit Statistics						
Source	Std. Dev.	R^2	Adjusted R^2	Predicted R^2	PRESS	
Linear	2.46	0.7110	0.6647	0.5599	230.81	Suggested
2FI	2.57	0.7603	0.6342	0.3844	322.86	
Quadratic	2.42	0.8324	0.6759	0.1087	467.42	

3.5.1 Response surface plotting for estimation of operating variables

The actual visual predicted percentage for CV, MB and MO removal is presented in Figure 7 & 8, it was found that the actual values for CV, MB and MO removal by SP-IONPs- ALG are well in line with the predicted values from the model equations (8), (9) and (10) respectively:

$$\mathbf{R}=+7.35271+13.44948pH+0.126083Time-0.424287Conc+524.20718Dose+0.170955pH*Time+0.030527pH*Conc-10.05182pH*Dose-0.002558Time*Conc+1.44948Conc*Dose-0.627519pH^2+0.013680Time^2+0.005338Conc^2+2717.30965Dose^2 \quad (8)$$

$$\mathbf{R}=+27.86285+7.17505*pH+0.147871*Time-0.292797*Conc+128.48359*Dose \quad (9)$$

$$\mathbf{R}=+82.91850+1.76262*pH+0.032311*Time-0.063977*Conc+28.07427*Dose \quad (10)$$

The three-dimensional (3D) response surface plots make available data on the interaction's terms and their effects on the dependent variable. Hither, each plot is created by varying two individual variables in their corresponding experimental range while keeping the two-parameter constant. Fig 9 demonstrate the interaction of adsorption operating parameters of pH (A), experimental time (B), concentration (C), and sorbent dosage (D) on removal efficiency for CV dye. It was clearly noted that the combination pH with initial concentration and contact time with adsorbent dosage have a positive impact on CV adsorption as said by contour lines and multiple regression as Equation (8). As seen in Figure (9 b), increase in initial pH from 4 to 10 with (t; 35 minutes and adsorbent dose 0.06 g) as constant leads to removal % increase,

because of higher performance of the sorbent in pH more than pH_{ZPC} (7.1) [54]. Fig. 9e, depicts the combined influence of the adsorbent dose and contact time with (C_0; 55 mg $L^{-1}$and pH 6) as constant, increase in removal % was observed with increasing in adsorbent dose and contact time together. Dye removal increased with increasing sorbent dose may be associated with more free sites on adsorbent molecules surface [55]. From these results were predicted that to pH 6, contact time 35minutes and adsorbent dosage 0.06 g, these consider optimal conditions for remove crystal violet with higher removal percentage (93.49%).

In Figure 10, determine the interaction of adsorption operating parameters of A, B, C, and D on removal efficiency for MB dye. The positive sign in pH, contact time and adsorbent dosage +7.17505, +0.147871 and +128.48359 respectively, indicated these parameters had positive effect in MB removal but initial concentration has negative effect according to (Eq. 9). Fig 10a represents combination of contact time and pH with (C_0; 55 mg L^{-1} and sorbent dosage; 0.06 g) as constant, these depicts increase in removal % with increasing contact time and pH together, these results similar to previous study recorded by Abdelilah et al. [56]. The interaction of adsorption parameter on removal MO illustrated in Fig 11, the highest positive sign with adsorbent dose (+28.07427) according to (Eq. 10) was explained highest effect of adsorbent dose and pH with (C0; 55 mg L^{-1} and t; 35 minutes) as constant which illustrated in Fig 11c. The results from three model for CV, MB and MO indicating that pH, contact time & sorbent dose have positive effect in removal percentage but dyes concentration has negative effect, these explained high removal percentage for CV, MB and MO (93.46%, 96.47% and 94.4%; respectively) in run 18 with pH equal 6, contact time 35 minutes and adsorbent dosage 0.06 g.

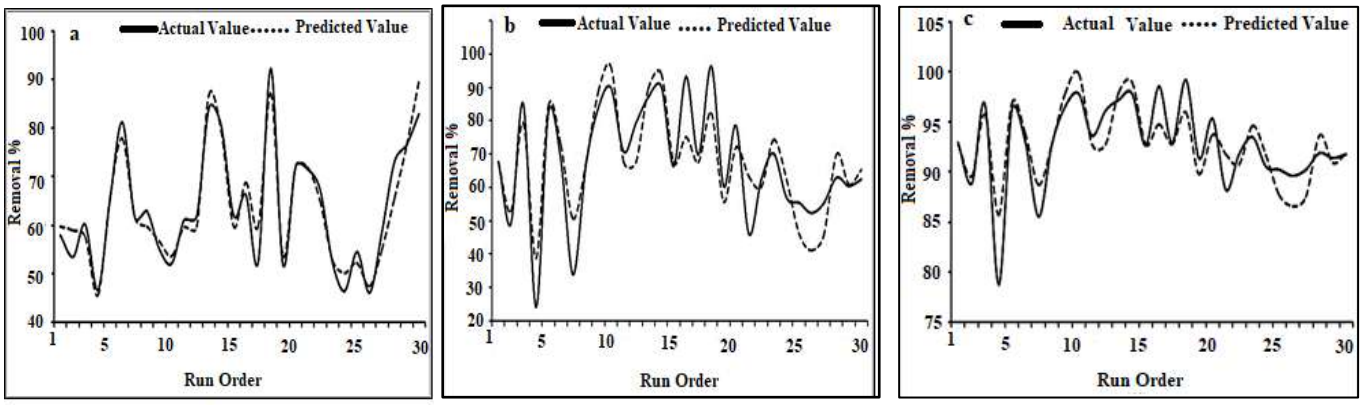

Figure 7. The predicted values v_s actual values, **(a)** Removal percentage of CV by SP-IONPs- ALG, **(b)** Removal percentage of MB by SP-IONPs- ALG, and **(c)** Removal percentage of MO by SP-IONPs- ALG

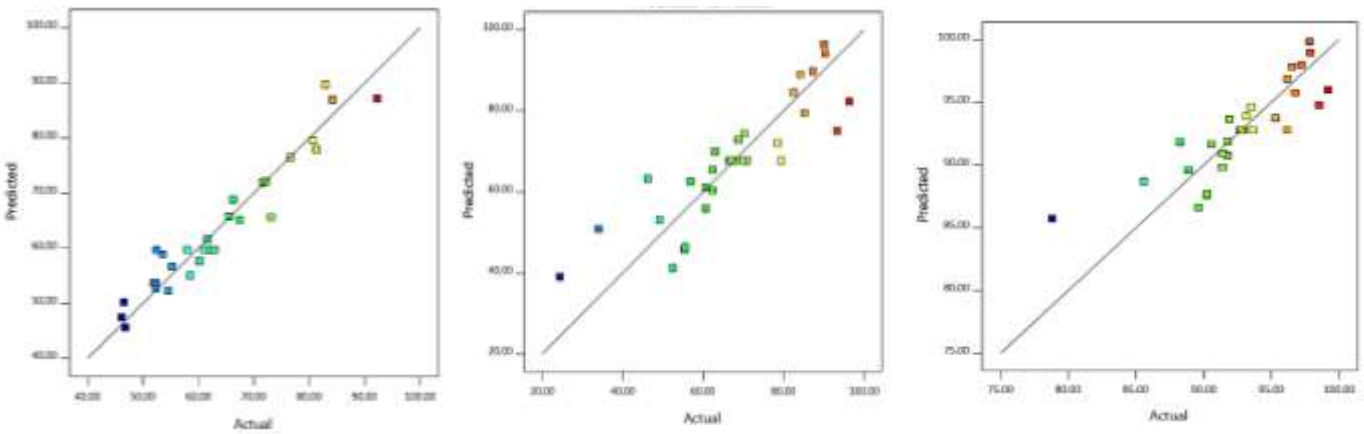

Figure 8. The predicted values v_s actual values, **(a)** Removal percentage of CV by SP-IONPs- ALG, **(b)** Removal percentage of MB by SP-IONPs- ALG, and **(c)** Removal percentage of MO by SP-IONPs- ALG.

3.6. Adsorption mechanism

CV, MB & MO adsorption in the SP-IONPs- ALG surface could be occurred from a amalgamation of several interactions: (I) electrostatic attractions of the positively charged in CV & MB dyes ions with the several carboxyl groups present in the SP-IONPs- ALG composite or negative charged of MO dye and hydrogen in of SP-IONPs- ALG hydroxyl groups according to pH of aqueous solution, (II) hydrophobic π–π stacking interactions occurred between the dyes aromatic rings and the SP-IONPs- ALG composite surface, (III) dipole–dipole H-bonding interactions [57].

3.7. SP-IONPs- ALG adsorbent regeneration

Adsorption of dyes from wastewater effluents from textile industries should own a good adsorption capacity, high stability and easy separation properties. The regeneration considered to be essential for the reason that it allows the recovery of the components present in the adsorbed phase and enables the reuse of the adsorbent [58]. The removal *%* (*R %*) of the adsorbent to CV, MB & MO are summarized in Table (5). HCl and NaOH have capabilities for desorbed (CV & MB) and MO respectively from SP-IONPs- ALG adsorbent. The desorption efficiency (R %) values were recorded 86.3, 85.9 and 86.2 % for CV, MB & MO respectively after fourth cycle. Consequently, it can be determined that HCl and NaOH are appropriate desorbing agents for CV, MB & MO from the adsorbent.

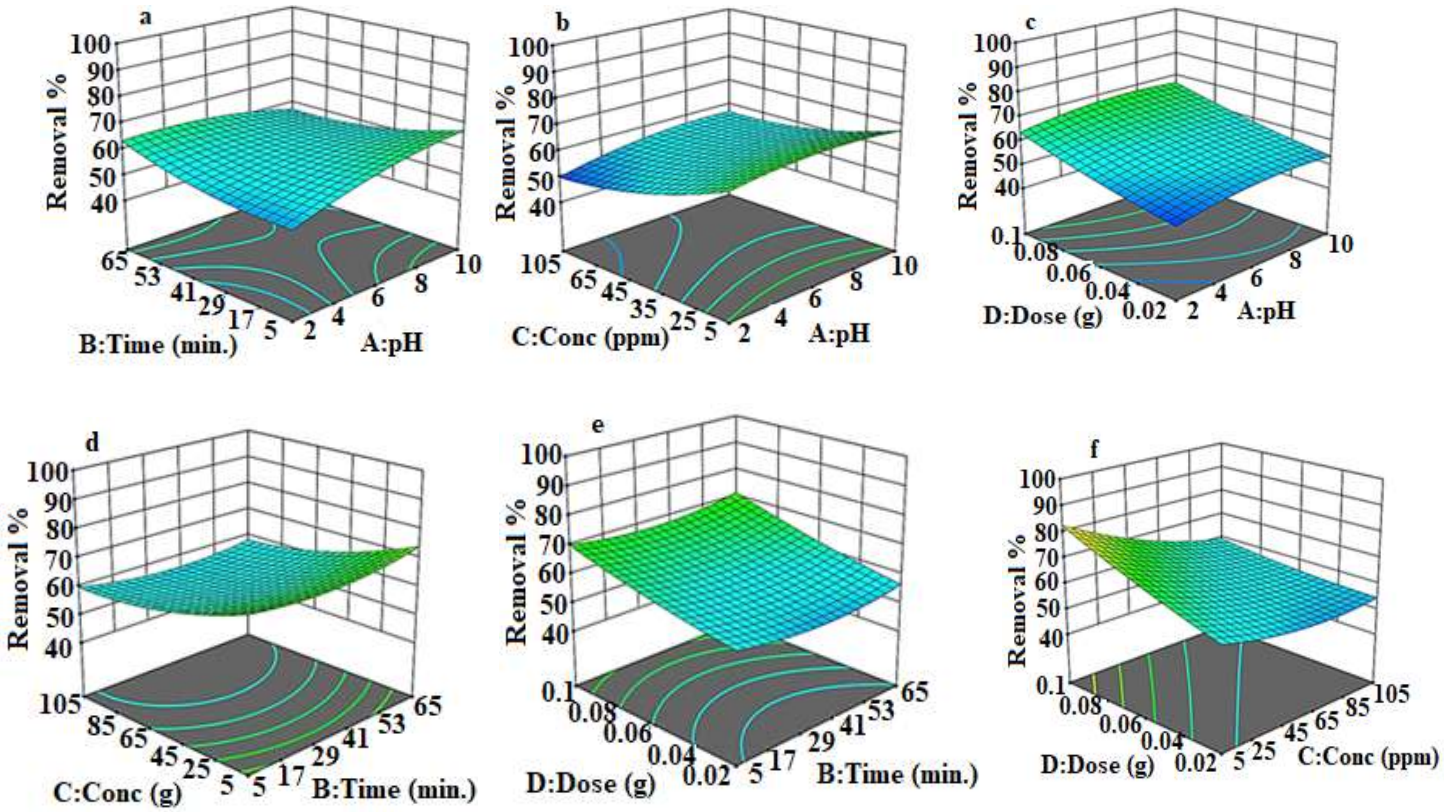

Figure 9. RSM 3D surface plots for adsorption of CV onto SP-IONPs- ALG **(a)** Effect of contact time and pH on CV removal (C0, 55 mg L-1 and adsorbent dose 0.06 g), **(b)** Effect of initial concentration and pH on CV removal (contact time 35 minutes and adsorbent dose 0.06 g), **(c)** Effect of adsorbent dose and pH on CV removal (C0, 55 mg L-1 and contact time 35 minutes), **(d)** Effect of initial concentration and contact time on CV removal (pH 6 and adsorbent dose 0.06 g), **(e)** Effect of adsorbent dose and contact time on CV removal (C0, 55 mg L-1 and pH 6), **(f)** Effect of adsorbent dose and initial concentration on CV removal (pH 6 and contact time 35 minutes).

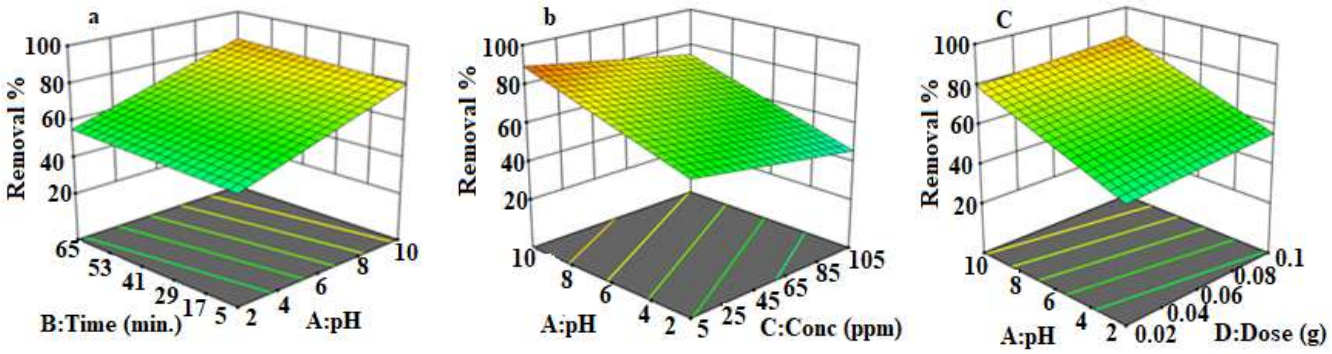

Figure 10. RSM 3D surface plots for adsorption of MB onto SP-IONPs- ALG **(a)** Effect of contact time and pH on MB removal (C0, 55 mg L^{-1} and adsorbent dose 0.06 g), **(b)** Effect of initial concentration and pH on MB removal (contact time 35 minutes and adsorbent dose 0.06 g), **(c)** Effect of adsorbent dose and pH on MB removal (C0, 55 mg L^{-1} and contact time 35 minutes).

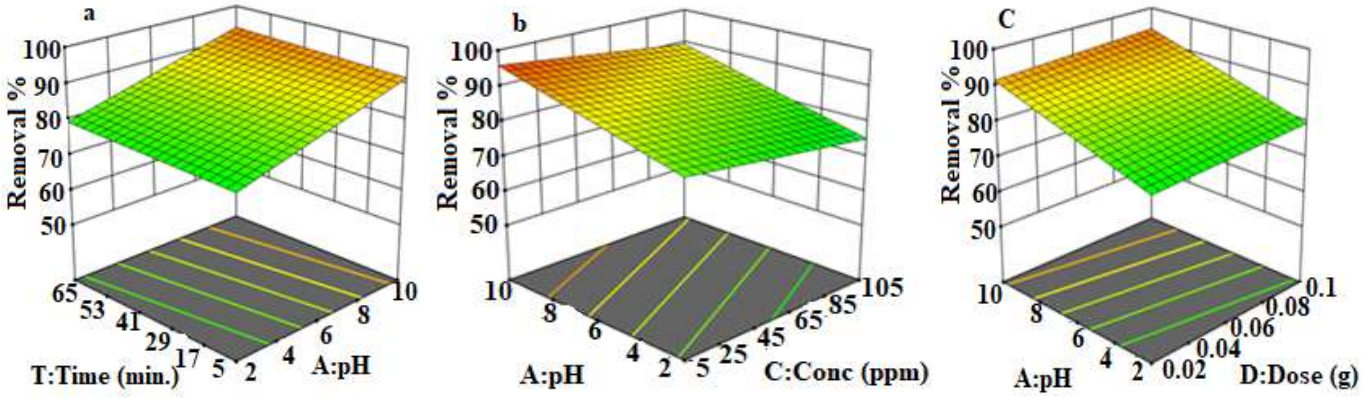

Figure 11. RSM 3D surface plots for adsorption of MO onto SP-IONPs- ALG **(a)** Effect of contact time and pH on MO removal (C0, 55 mg L^{-1} and adsorbent dose 0.06 g), **(b)** Effect of initial concentration and pH on MO removal (contact time 35 minutes and adsorbent dose 0.06 g), **(c)** Effect of adsorbent dose and pH on MO removal (C0, 55 mg L^{-1} and contact time 35 minutes).

Table 5. Reusability study of SP-IONPs- ALG adsorbent

	Crystal violet (CV)		Methylene blue (MB)		Methyl orange (MO)	
Adsorbent cycles	**Amount of adsorbent**	**Removal %**	**Amount of adsorbent**	**Removal %**	**Amount of adsorbent**	**Removal%**
First adsorption	0.05	95.5	0.05	95	0.05	96.7
Cycle 1	0.052	91.3	0.049	93.2	0.05	95.3
Cycle 2	0.050	89.1	0.046	90.32	0.049	94.2
Cycles 3	0.049	86.8	0.044	87.4	0.048	89
Cycles 4	0.049	86.3	0.044	85.9	0.047	86.2

4. CONCLUSION

In the present study, we succesfuly produced SP-IONPs- ALG by using green iron oxide nanoparticles using *Spirulina platensis*. The morphology, size and chemical compassion of the prepared SP-IONPs- ALG were investigated by using SEM and EDX and PH_{PZC} measurement. RSM used to investigate the efficiency of SP-IONPs- ALG to adsorption of CV, MB and MO dyes from aqeoues solution. The effects of

operational parameters studied by using. A 2^4 (CCD) based on single- factor experiments and a four-variables, pH (x_1), experimental time (x_2), initial dyes concentration (x_3) & adsorbent dose (x_4) to evaluate the efficiency of SP-IONPs- ALG for adsorption of CV, MB and MO from aqueous solution. pH, contact time and adsorbent dosage had positive effect in dyes removal percentage with high removal percentage for CV, MB and MO (93.46%, 96.47% and 94.4%; respectively). Freundlich model was more fit for the description CV & MB adsorption with (Q_{max}) equal 344.82 mg g^{-1}, 416.6 mg g^{-1} respectively but Langmuir isotherm better than Freundlich model to experimental data for representing the adsorption process of MO with maximum adsorption capacity 370.3 mg g^{-1}. Kinetic profile close-fitting to PSORE. Moreover, the recyclability test of SP-IONPs- ALG was efficiently conducted up to 4 times of adsorption/desorption cycles using the desorbing agent of 0.1 M HCl for (CV and MB) and 0.1 M NaOH for MO. This study presents an eco-friendly adsorbent (green SP-IONPs- ALG) for removal CV, MB and MO dyes from aqueous solution and determined their efficiency by using RSM methodology. .

REFERANCES

[1] Manel, W., Besma, Kh. and Féthi, Z. *Environmental Science and Pollution Research,* 26: 18942, 2018, 10.5802/crchim.41.

[2] Bhattacharya, S., Gupta, A.B., Gupta, A. and Pandey, A. *Water remediation.* Singapore, Springer, 3–8, 2018, doi: 10.1007/978-981-10-7551-3_1.

[3] Priya, A., Kumar, Sh., Balbir, S. K., Vaishali, T., Jaspreet, K. B., Nisha, Sh., Sakshi, B. and Sagar, Panchal. International Journal of Biological Macromolecules, 129, 214-226, 2019, 10.1016/j.ijbiomac.2019.02.034.

[4] Douglas, G. B., Lurling, M., and Spears, B. M. *Water Res,* 97,4754, 2016, 10.1016/j.watres.2016.02.005.

[5] Li, R., Morrison, L., Collins, G., Li, A., and Zhan, X. *Water Res*, 96, 32–41, 2016, doi: 10.1016/j.watres.2016.03.034.

[6] Zhu, G., Wang, Q., Yin, J., Li, Z., Zhang, P. and Ren, B. *Water Res,* 05.035, 2016, 10.1016/j.watres.2016.05.035.

[7] Mittal, A. *J. Colloid Interf. Sci*, 343, 463–473, 2010, 10.1016/j.jcis.2009.11.060.

[8] Nasrin, B., Mohammad, A., Jadidi, K., Amir, S., Ali, M. and Amani, S. T. *Applied Physics*, A 124:363, 2018, doi.org/10.1007/s00339-018-1782-3.

[9] Ebrahiminezhad, A., Zare-Hoseinabadi, A., Sarmah, A.K., Taghizadeh, S., Ghasemi, Y. and Berenjian, A. *Mol. Biotechnol*. 60(2), 1–15, 2017, 10.1007/s12033-017-0053-4.

[10] Palagiri, B., Chintaparty, R., Nagireddy, R.R. and Imma, *V.S.R Phase Transit*, 90(6), 578–589. 2017, doi:10.1080/01411594.2016.1237636.

[11] Orsini, N.J., Babić-Stojić, B., Spasojević, V., Calatayud, M., Cvjetićanin, N. and Goya G. J. *Magn. Mater*, 449, 286–296, 2018, 10.1016/j.jmmm.2017.10.053.

[12] Kastrinaki, G., Lorentzou, S., Karagiannakis, G., Rattenbury, M., Woodhead, J. and Konstandopoulos, *A. J. Aerosol Sci*, 115, 96–107, 2018, doi:10.1016/j.jaerosci.2017.10.005.

[13] Salunke, B. K., Sawant, S.S., Lee, S.I. and Kim, B.S. *Appl Microbiol Biotechnol*, 99(13) 5419–542, 2016, 10.1007/s11274-016-2044-1.

[14] Yaquan, W., Yi, F., Xiong-Fei, Z., Xingguang, Z., Jinlong, Jiang. and Jianfeng, Yao. *Journal of Colloid and Interface Science*,514,190-198, 2018, 10.1016/j.jcis.2017.12.035.

[15] Jung, W. S, J. *Ind. Eng. Chem*, 26, 364–369, 2015, doi:10.1016/j.jiec.2014.12.010.

[16] Drumm, F.C., Franco, D.S.P.,Grassi, P. *Environ Technol*, 1–12, 2021, 10.1080/09593330.2021.1881828.

[17] Li, Z., Sellaoui, L., Gueddida, S. *J Mol Liq*, 319:114348, 2020, doi.10.1016/j.molliq.2020.114348.

[18] Boukhemkhem, A. and Rida, K. *Adsorption Science and Technology*, 35,(9-10), 2017, doi.10.1177/0263617416684835.
[19] Dai, H., Huang, Y., Huang, H. *Carbohydr Polym*, 185:1–11, 2018, doi: 10.1021/acsapm.0c00831.
[20] Garbaa, Z.N., Rahima, A. A. and Belloc, B. Z. *J Environ Chem Eng*, 3:2892–2899, 2015, 10.1016/j.jece.2015.10.017.
[21] Ünügül, T., Nigiz, F.U. *Arab J Sci Eng*, 2021, doi: 10.1007/s13369-021-05905-z .
[22] Das, P., Banerjee, P. and Mondal, S. *Environ Sci Pollut Res*, 22:1318– 1328, 2015, doi:10.1007/s11356-014-3419-1.
[23] Zeynep, C., Gürkan, K., Berna, E., Erdem, A. *Journal of Molecular Structure*, 1224, 15, 129182, 2020, 10.1016/j.molstruc.2020.129182.
[24] Shalaby, M. Sh., Madkour, F. F., EL-Kassa, Y. H., AMER, A. and Elkharhy, M. A. *Environmental Science and Pollution Research*, 2021, 10.1007/s11356-021-15544-4.
[25] EL-kassa, H. Y., Aly-Eldeen, M. A. and Gharib, S. *Acta Oceanol*,35(8): 89–98, 2016, doi:10.1007/s13131-016-0880-3.
[26] Samrot, A. V., Ali, H.H., Selvarani, A.J., Etel, F., Raji .P., Prakash, P., Suresh, S. K., *Curr Res Green Sustain Chem*, 4:100066, 2021, doi.10.1016/j.crgsc.2021.100066.
[27] Hurairah, S.N., Lajis, N.M., Halim, A.A. *GEP*, 08(02):128–14, 2020, 10.4236/gep.2020.82009.
[28] Bing, L., Qian, W., Jian-Zhong, G., Wei-Wei, H. and Li, Liua, *Bioresource Technology*, 268, 454–459. 2018, doi.org/10.1016/j.biortech.2018.08.023.
[29] Samarghandi, M. R., Nemattollahi, D., Asgari, G., Shokoohi, R., Ansari, A. and Dargahi, A. *Sep Purif Technol*, 54(4):478–493, 2019, 10.1080/01496395.2018.1512618.
[30] Dargahi, A., Mohammadi, M., Amirian, F., Karami, A. and Almasi, *ADesalin Water Treat*, 87: 199–208, 2017, 10.5004/DWT.2017.21064.
[31] Langmuir, I. *American Chemical Society*, 40, 1361–1403. 1918, doi: org/10.1021/ja02242a004.
[32] Freundlich, H. Z, *Phys Chem*, 57U:385–470, 2017, doi: 10.1515/zpch-1907-5723 .
[33] Lagergren, S. Kungl Svenska Vetenskapsakad. *Handl*, 24, 1–39, 1898, doi: 10.1002/andp.18983000208.
[34] Ho, Y.S. and McKay G. *Process Bio*, 34, 451–465, 1999, doi:10.1016/S0032-9592(98)00112-5.
[35] Kazak, O., Eker, Y.R., Akin, I., Bingol, H. and Tor, A. *J. Environ. Chem. Eng*. 5, 2639–264, 2017, doi: 10.1016/j.jece.2017.05.018.
[36] Zakaria A., AbdallahA., Abdellah A., Mohamed, Zbair, Hassan, A., NoureddineEl Alem Chemosphere, 236:124351, 2019, doi.10.1016/j.chemosphere.2019.124351.
[37] Xiaoshu, L., Guangming, J., Xiaoqin, X., Donglei, W., Tiantian, Sheng., Chen, Sun. and Xinhua, Xu. 417,748-758, 2013, doi: 10.1016/j.jhazmat.2013.09.036.
[38] Soheila. H., Marzieh. T. and Seyed. J. S, *Journal of Environmental Health Science & Engineering*, 13:8, 2015, doi.org/10.1186/s40201-015-0156-4.
[39] Rigueto, C.V.T, Piccin, J. S., *AEcol Eng* 150:105817, 2020, 10.1007/s42452-021-04736-9.
[40] Hossein, H. and Khadijeh, AJ, *Inorg Organomet Polym*, 27:1595–1612, 2017, 10.1007/s10904-017-0625-6.
[41] Ting, L. and Beigang, L. *Water Journal of Polymers and the Environment*, 29:1576–159., 2021, doi:10.1007/s10924-020-01977-4.
[42] Gil, A., Amiri, M. J., Abedi-Koupai, J. and Eslamian, S, *Environ Sci Pollut Res*, 25, 2814–2829, 2018, doi: 10.1007/s11356-017-0508-y.
[43] Chan, A.W. and Neufeld, *R.J. Biomaterials*, 30 6119-6129, 2009, doi: 10.1016/j.biomaterials.2009.07.034.
[44] Khalil, A., Aboamera, N. M., Nasser, W.S., Mahmoud, W. H. and Mohamed, G. G. J. S. *Separation and Purication Technology*, 224:509–514, 2019, doi: 10.1016/j.seppur.2019.05.056.
[45] Noreen S, Khalid U, Ibrahim SM, Javed T, Ghani A, Naz S, Iqbal M. *J Mater Res Technol*, 9(3):5881–5893, 2020, doi: 10.1016/j.jmrt.2020.03.115.

[46] Anjali, A. E., Emad, A. and Fawzi, B, *International Journal of Greenhouse Gas Contro*l, 83, 117-127. . 2019, doi: 10.1016/j.ijggc.2019.02.005.

[47] Mahsa, B., Vahid, J. and Javad, E. *Biomac*, S0141-8130(18)30736-0, 2017, doi: 10.1016/j.ijbiomac.2018.05.012.

[48] Miandad, R., Kumar, R., Barakat, M. A., Basheer, C., Aburiazaiza, A. S., Nizami, A. S and Rehan, M. *Journal of Colloid and Interface Science*, 511, 402–410, 2018, doi: 10.1016/j.jcis.2017.10.029.

[49] Pathania, D., Sharma, S. and Singh, P. *Arabian Journal of Chemistry*, 10, S1445–S1451, 2017, doi: 10.1016/j.arabjc.2013.04.021.

[50] Nadia, B., Mokhtar, B., Nassima, D. and Ani, I. *International Journal of Biological Macromolecules*, S0141-8130(18)33769-3, 2018, doi: 10.1016/j.ijbiomac.2018.11.102.

[51] Shalaby, M. S, Madkour, F. F., El-Kassas, H. Y., Mohamed, A. A. & Elgarahy, A. M. International *Journal of Phytoremediation*, 2021, doi: 10.1080/15226514.2021.1984389.

[52] Mohammad, F., Meisam, Sh. and Fezzeh, A. *Journal of the Iranian Chemical Society*, 15:733–74, 2018, doi: 10.1007/s13738-017-1273-z.

[53] Priya, A., Kumar, Sh., Balbir. S. K., Vaishali, T., Jaspreet, K. B., Nisha, Sh., Sakshi, B. and Sagar, P, *International Journal of Biological Macromolecules*, 129, 214- 226, 2019, doi: 10.1016/j.ijbiomac.2019.02.034.

[54] Marrakchi, F., Hameed, B.H., Hummadi, E.H. *Int J Biol Macromol*, 163:1079–1086, 2020, doi: 10.1016/j.ijbiomac.2020.07.032.

[55] Ali, S. and Ebrahim, N.K. Adsorption, 24:647–666, 2018, doi.10.1007/s10450-018-9972-z.

[56] Abdelilah, E., Nouh, A., Abdelghani, H., Zeeshan, A., Mohamed, L., Mahmoud, El., Abdelaziz, A. A., Rajae, L. and Abdallah, A., *Journal of Dispersion Science and Technology*,52,21-12602-12611, 2020, doi:10.1080/01932691.2020.1857263.

[57] Asma, E., Fawzi, B., Munirasu, S. and Mohammad, A. H. Polym. Bull, 76:175–203, 2019, doi.10.1007/s00289-018-2378-y.

[58] Cechinel, M.A.P., Mayer, D.A., Mazur, L.P., Silva, L.G.M., Girardi, A., Vilar, V.J.P., de Souza, A.A.U., Selene, S.M.A, *J Clean Prod*. 172: 1928–1945, 2018, 10.1016/j.jclepro.2017.11.235.